TOPOGRAPHY-DEPENDENT MOTION COMPENSATION: APPLICATION TO UAVSAR DATA

Cathleen E. Jones, Scott Hensley and Thierry Michel
Jet Propulsion Laboratory, California Institute of Technology
4800 Oak Grove Drive, Pasadena, CA 91109
Email: cathleen.jones@jpl.nasa.gov

ABSTRACT

The UAVSAR L-band synthetic aperture radar system has been designed for repeat track interferometry in support of Earth science applications that require high-precision measurements of small surface deformations over timescales from hours to years. Conventional motion compensation algorithms, which are based upon assumptions of a narrow beam and flat terrain, yield unacceptably large errors in areas with even moderate topographic relief, i.e., in most areas of interest. This often limits the ability to achieve sub-centimeter surface change detection over significant portions of an acquired scene. To reduce this source of error in the interferometric phase, we have implemented an advanced motion compensation algorithm that corrects for the scene topography and radar beam width. Here we discuss the algorithm used, its implementation in the UAVSAR data processor, and the improvement in interferometric phase and correlation achieved in areas with significant topographic relief.

I. UAVSAR OVERVIEW

Synthetic aperture radar systems have been used for many years to measure surface deformation using repeat track, or differential, interferometry (DifInSAR). Differential interferometry measures the coherent phase difference between complex SAR imagery of the same location collected at two different times. Surface deformation between the two passes results in a phase change in the interferometric signal. The accuracy of DifInSAR is limited by changes to the interferometric phase between the two tracks that are not associated with a change in the surface. The dominant sources of interferometric phase error are changes in the look direction or distance to a target on the surface, which arise mainly from platform position and attitude differences between the two flight tracks of the interferometric pair. A change in the look direction leads to decorrelation between the two images, reducing the phase coherence that is required for interferometry to be applicable. In addition, when the platform position differs between the two passes, i.e., when there is a nonzero repeat track baseline, an interferometric phase component is introduced that depends upon the surface topography in addition to the phase component attributable to surface change. Because both of these problems are exacerbated on airborne platforms, which are subject to variable wind conditions, satellite-based SAR systems have been mainly used for DifInSAR.

UAVSAR is a new airborne NASA asset for PolSAR and high-precision DifInSAR measurements. The system is instrumented with a quad-polarization, phased array, L-band radar antenna and deployed on a Gulfstream-3 aircraft. The radar is mounted in a pod below the aircraft fuselage so that it can be ported to alternate platforms in the future. More information about the radar design parameters is included in Table I and a description of the hardware can be found in [1]. The UAVSAR instrument has been designed to monitor surface deformation to sub-centimeter accuracy with 10 m x 10 m surface area resolution, a scale unattainable by satellite-based SAR instruments. The radar electronics has internal calibration signal paths to compensate instrumental phase drifts so that in the absence of external error sources the phase can be corrected with sufficient accuracy to monitor line-of-sight change to 3 mm accuracy. To achieve this level of accuracy in the derived surface deformation requires very accurate determination of the platform motion, attitude, and location, which is provided by a differential GPS system and a high-precision inertial navigation unit. The information about the platform motion is used to minimize decorrelation between the acquired data sets by making real-time adjustments to the track position and the antenna beam steering angle during radar data collection in order to avoid the error sources associated with changes in the repeat track baseline and the look direction.

To reduce the repeat track baseline, the Gulfstream-3 platform has been modified to accept input from a precision autopilot system (PPA) designed to maintain the flight path within a tube of 10 m diameter about the planned flight track over 90% of the time under conditions of light turbulence or less [2]. Information from the differential GPS system, which locates the platform position to submeter real-time accuracy, is fed to the PPA, which commands the Instrument Landing System to alter the aircraft control surfaces in order to maintain the desired track. In practice, the desired flight track is maintained within the 10 m diameter tube well over the required 90% of the time. An example of the track error statistics collated over nearly 10 hours of radar data collection is shown in Figure 1. Typically the PPA maintains the track within a 5 m diameter tube 95% of the time.

Aircraft attitude angles differ between flights due to different wind conditions. Both yaw and pitch changes alter the look direction, and even during the same flight, the yaw can vary on a short timescale because of turbulence and the pitch angle of the aircraft changes as the fuel load changes. Even in the

TABLE I
RADAR PARAMETERS

Parameter	Value
Frequency	1.26 GHz (.2379 m)
Bandwidth	80 MHz
Pulse Duration	5-50 μs
Polarization	Quad Polarization
Range Swath	16 km
Look Angle Range	$25° - 65°$
Transmit Power	3.1 kW
Antenna Size	0.5m $\times$ 1.6 m
Operating Altitude Range	2000-18000 m
Ground Speed Range	100-250 m/s

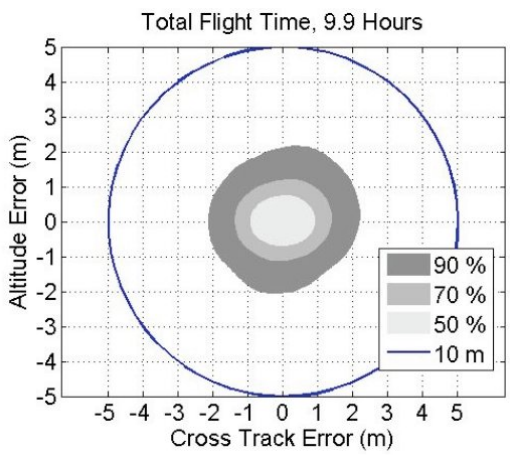

Fig. 1. *Statistics quantifying the ability of the Precision Autopilot control system to maintain the flight track of the UAVSAR Gulfstream-3 platform within a tube centered on the planned flight track. The flight track lies within a 4 m diameter tube approximately 90% of the time. The data is compiled over 9.9 hours of radar data acquisition.*

absence of these effects, small yaw, pitch, and roll changes are introduced by the PPA, which varies the platform attitude to maintain the flight track. Therefore, in practice during a flight line the attitude angles vary periodically on a timescale comparable to the synthetic aperture time. To actively adjust the look angle, the radar control flight software continually monitors the platform attitude, velocity, and heading, adjusting the phase of individual elements of the phased-array antenna to steer the beam to within $0.2°$ of the user-specified squint angle.

II. MOTION COMPENSATION

The highly accurate ephemeris and attitude information used for real-time flight path control and antenna beam steering is essential for post processing the SAR image data. Data from the differential GPS and INU are blended post-flight in the ground data system to generate the position and attitude data used to process the SAR data. At this stage, the platform position is determined to 2-3 cm accuracy. To achieve sub-centimeter level accuracy in the surface deformation derived from the interferometric phase requires appropriate motion compensation to remove the platform-induced phase changes.

For repeat pass processing, both tracks are processed to the same reference track, which is chosen to maximize the spectral overlap of the signals from the two tracks. The normal flow of the UAVSAR data processor is to perform the following steps on each patch, or synthetic aperture, of data, (1) range compression; (2) presum, i.e., resampling of the signal to a uniform along-track spacing; (3) motion compensation of each track to a track-specific reference path; (4) range migration; (5) azimuth compression; (6) motion compensation to the common reference track; and (7) reskewing of the data from individual patches to a common perspective. This process forms the single-look complex (SLC) image for each track. The repeat pass interferogram is formed by multiplying the complex value of one image by the complex conjugate of the second image; the phase of the interferogram contains the surface deformation information, plus a term dependent upon the scene topography when the tracks are flown with nonzero baseline.

During the motion compensation steps, the phase and range of the signal are corrected for the baseline offset between the actual flight track and the desired reference track, i.e., for the difference between the actual platform position and the position at which a target at the same slant range would be imaged on the reference track. The goal of motion compensation is to correct for the component of the baseline along the look direction to the target, which affects both the slant range and the phase of the signal. The range shift depends upon the baseline, $\vec{b}$, and the look direction, $\hat{\rho}$, as

$$\Delta\rho = \vec{b} \cdot \hat{\rho}. \tag{1}$$

Errors in the motion compensation phase and range corrections arise from errors in the either the baseline or look direction determination.

The UAVSAR conventional motion compensation algorithm corrects for a nonzero baseline based upon several inaccurate assumptions: (1) The terrain imaged is all at the same height, the "reference height," which is taken to be the average height across the synthetic aperture; (2) the azimuth beam width is neglected in considering the radar return to originate entirely from beam center, the direction of peak antenna power; and (3) the look direction as a function of slant range is calculated based upon the average platform attitude angles across the patch and the antenna position at the center of the patch. Each of these assumptions leads to errors in the estimated look direction, which in turn result in phase errors that mask the surface change signal in areas with even moderate surface height changes or conditions where the attitude angles vary significantly across the synthetic aperture, leading to both image defocussing in the along-track direction and a relative shift between the final processed images from the two different passes.

Advanced motion compensation algorithms that take into account topography and beam width have been developed previously. A review and comparison of several Fourier-based motion compensation algorithms is given in [3]. We have implemented a similar Fourier-based motion compensation algorithm that works on small, overlapping blocks of data and is implemented following the first motion compensation step.

In addition, the common track motion compensation is done using the actual terrain height instead of the reference height. We focus on determining the look direction more accurately based upon the true terrain height and the local attitude angles, using azimuth look direction information derived from doppler subbanding to account for the radar beam width. Our algorithm uses the attitude angles for the center of the block and the terrain height derived from a digital elevation model (DEM) instead of the average values across the patch. The results shown here are for a block size of 64, with linear feathering in the 16-line overlap region. The data in a patch is divided into blocks and each block is transformed from the slow time domain to the azimuth (along-track) frequency domain. The azimuth angle θ_a for the signal in a particular bin is determined from the azimuth frequency, f_a, of the bin and the radar wavelength, λ, as

$$\theta_a = \sin^{-1}\left(\frac{f_a \lambda}{2}\right). \tag{2}$$

This information is used to determine the look direction to the ground associated with a given platform position (taken as the position at block center), slant range, and azimuth angle for the particular doppler frequency bin. The look vector $\hat{\rho}$ for a given slant range ρ and azimuth angle θ_a is the intersection between the doppler cone with generator angle $\frac{\pi}{2} - \theta_a$, a sphere of radius ρ and the DEM elliposoid. The intersection location is determined numerically by minimizing the set of three equations

$$\hat{\rho} \cdot \hat{v} - \sin\theta_a = 0 \tag{3}$$

$$\hat{\rho} \cdot \hat{\rho} - 1 = 0 \tag{4}$$

$$(\vec{P} + \rho\hat{\rho}) \cdot (\vec{P} + \rho\hat{\rho}) - (r_e + h)^2 + \\ 2r_e(r_e + h)e^2 \sin^2 T_\lambda - r_e^2 e^4 \sin^2 T_\lambda = 0 \tag{5}$$

where e and r_e are the DEM ellipsoid eccentricity and semi-major axis radius, $\vec{P}$ and $\hat{v}$ are the position of the antenna phase center and the platform velocity direction at the center of the block, and T_λ and h are the latitude and height taken the DEM. The minimization is iterated until the value of h for the intersection of the ellipsoid and the doppler cone agrees with the height from the DEM. In general in regions with significant topographic relief the intersection point is not a single-valued function. In this case, the look vector is taken to be the closest intersection point in the cross-track direction that is also on a slope facing towards the radar platform, i.e., that is less likely to be in shadow.

Once the look vector, $\hat{\rho}$, is determined, the signal is corrected by a phase shift of

$$\Delta\Phi = \frac{4\pi\left(\vec{b} \cdot \hat{\rho} - \Delta\rho_{mc}\right)}{\lambda} \tag{6}$$

where $\Delta\rho_{mc}$ is the conventional motion compensation correction applied earlier. The data is also shifted in range to register the data relative to the reference track. Each element in the block is corrected to the look direction for its particular slant range and azimuth direction, which corrects for topography, attitude angle variations, and the beam aperture at the same time.

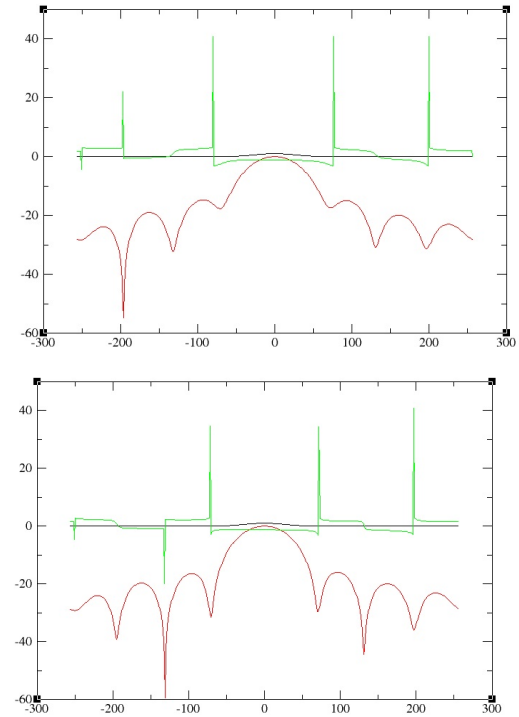

Fig. 2. *Azimuth impulse response for a point target with convention motion compensation (upper plot) and the advanced motion compensation (lower plot). The red curve is the amplitude and the green the phase of the response. In this instance the simulation for the point target included no topographic error, so the plot reflects the improved azimuth resolution from the aperture-dependent correction only.*

III. APPLICATION TO UAVSAR DATA

The topography and aperture dependent motion compensation algorithm was tested on both point target simulation data and UAVSAR data collected in California and Washington states in 2008. Here we show several test cases that demonstrate the improvement over the conventional motion compensation algorithm. A correction for the atmosphere has been applied in the analysis.

Simulated point target data was used to quantify the improvement in the image focus in the azimuth direction that results from accounting for the UAVSAR azimuth beam width of $8°$. The improvement is shown in Figure 2, where the top figure shows the azimuth impulse response with convention motion compensation and the bottom figures includes the aperture correction in the advanced motion compensation. In the simulated case no terrain topography was included. The azimuth focussing is clearly improved - the first null is deeper, the phase across the main lobe is flatter, and the PSLR is increased.

To show the effect of including topography, the advanced motion compensation was applied to UAVSAR data collected over Mt. St. Helens, Washington, on two passes separated in time by four hours. The tracks were flown at a heading of

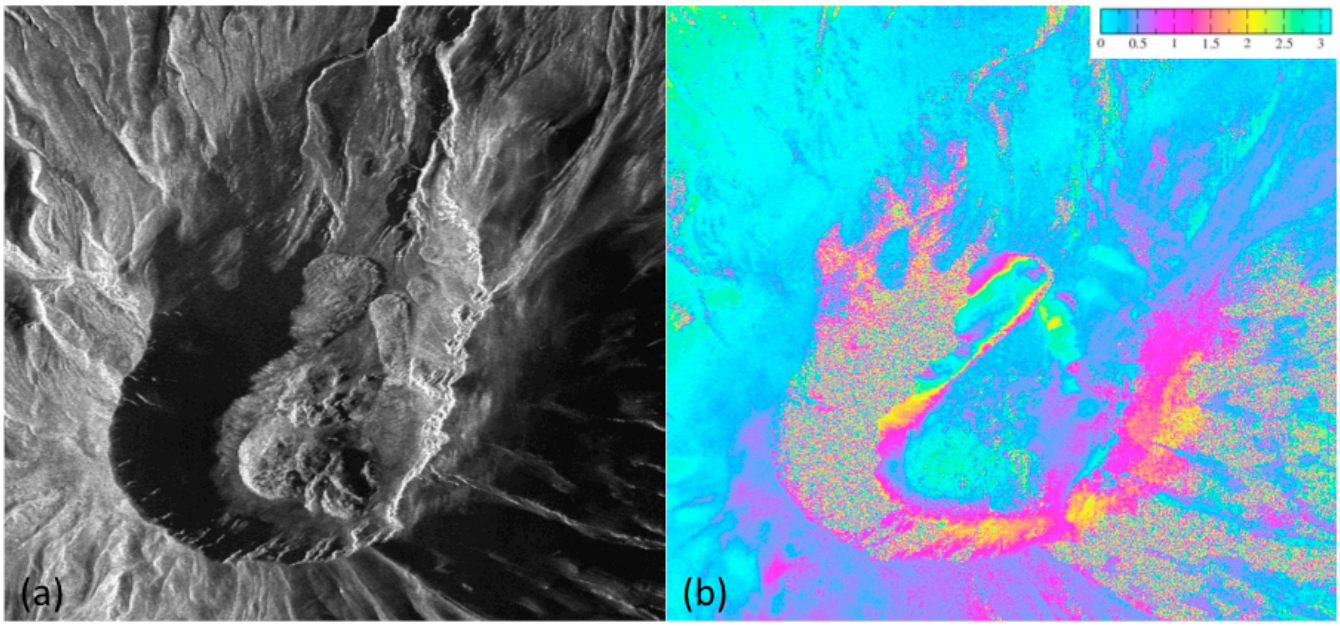

Fig. 3. *Interferogram of Mt. St. Helens caldera processed with the topography and aperture dependent motion compensation algorithm. The amplitude is shown in (a) and the phase is shown in (b). The phase wrap in (b) is set at π radians. The dome is seen at the bottom of the image with two large glaciers shown above that.*

181°. Figure 3 shows the interferometric amplitude and phase in the vicinity of the caldera. Motion of the glaciers within the caldera that occurred during the four hour interval can be seen in the image. Figure 4 shows the difference between the interferograms and the repeat pass image correlation for conventional and advanced motion compensation. The advanced algorithm removes many artifacts in the interferometric phase, shown in the upper two plots, greatly improving the repeat pass phase determination. A small phase discontinuity is visible at the patch boundary of the data processed with the advanced algorithm (plot (c), below the caldera); work continues to resolve this issue. Figure 4 also shows the improvement in the image correlation between the two passes. The histogram of the correlation statistics is shown in Figure 5; it can be seen that there is a significant shift towards higher correlation with the advanced algorithm.

The algorithm was also tested over a flat area in the Mojave Desert near Rosamond, California where the platform motion was sufficiently large as to introduce significant artifacts into the repeat pass interferogram when processed with conventional motion compensation. In this case the terrain does not account for the phase artifacts in the interferogram, so this tests the beam aperture correction of the advanced algorithm on real data. Figure 6 shows the interferograms for the two motion compensation algorithms. The phase bands in the along-track direction that remain with regular motion compensation and are most clear in the near range correlate with the yaw motion of the aircraft. The advanced motion compensation removes almost all of these artifacts. The small phase gradients remaining in the advanced motion compensated image probably result primarily from small, unmeasured motion that causes residual errors in the baseline determination. In this case, the phase

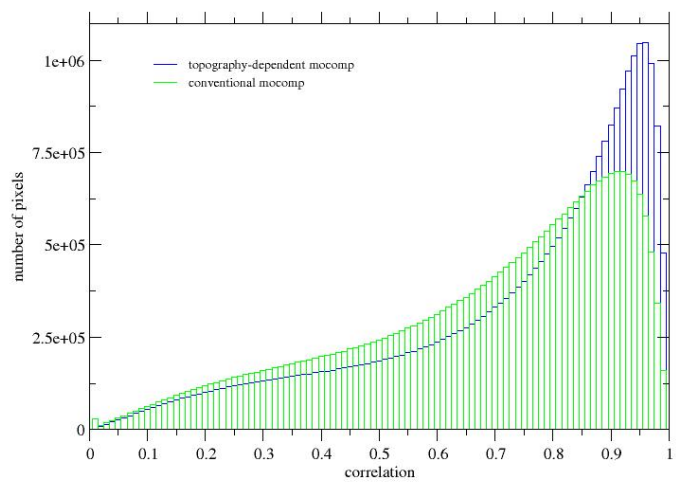

Fig. 5. *Correlation statistics for DifInSAR images of the area around Mt. St. Helens. The histogram of the correlation statistics is shown in green for conventional motion compensation and in blue for the advanced topography and beam aperture dependent motion compensation algorithm.*

artifacts in conventional motion compensation arise from both the narrow beam approximation and because the yaw angle varied significantly from the average values across a synthetic aperture, leading to errors in the calculated look direction.

IV. CONCLUSIONS

Motion compensation that accounts for topography and beam aperture effects are clearly needed for the UAVSAR repeat pass interferometry to produce high precision, accurate estimates of surface deformation. The algorithm implemented

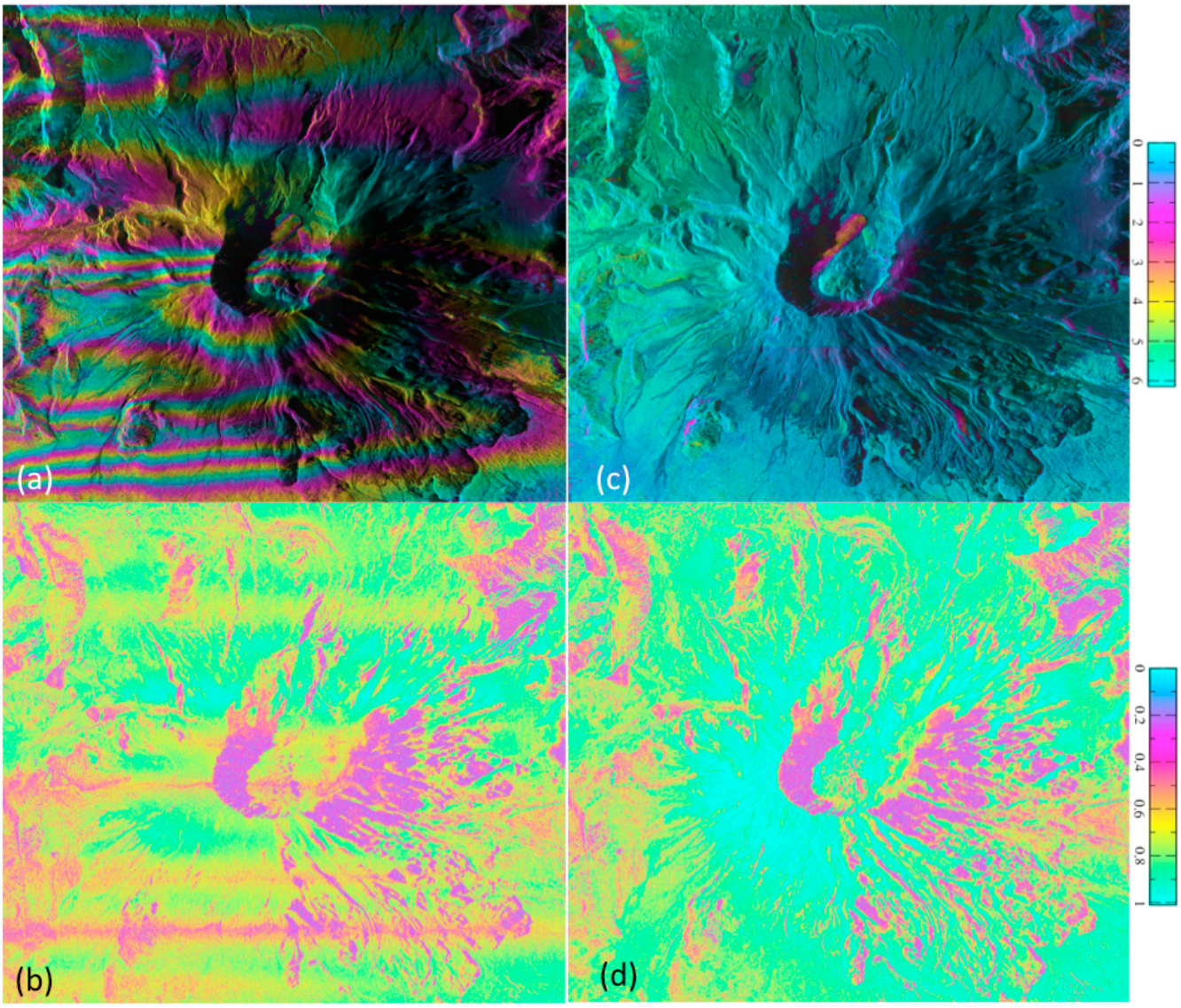

Fig. 4. *Repeat pass interferograms (top) and correlation maps (bottom) of the Mt. St. Helens area processed with the conventional motion compensation algorithm [(a) and (b)] and the advanced topography and aperture dependent motion compensation algorithm [(c) and (d)]. The phase wrap for the interferogram is set at* 2π *radians.*

corrects for both leading to a significant improvement in the repeat pass interferometric products.

ACKNOWLEDGMENT

This research was conducted at the Jet Propulsion Laboratory, California Institute of Technology, under contract with the National Aeronautics and Space Administration.

REFERENCES

[1] Scott Hensley *et. al.* The UAVSAR Instrument: Description and First Results. In the *Proceedings of the 2008 IEEE Radar Conference, Rome, Italy, May 26-30, 2008.*

[2] James Lee, Brian Strovers, and Victor Lin. C-20A/GIII Precision Autopilot development in support of NASAs UAVSAR program. In *Proceeding of the NASA Science Technology Conference 2007*, Greenbelt, Maryland, June 2007. NASA.

[3] Pau Prats, Karlus A. Camera de Macedo, Andreas Reigber, Rolf Scheiber, and Jordi J. Mallorqui. Comparison of Topography- and Aperture-Dependent Motion Compensation Algorithms for Airborne SAR. IEEE Geoscience and Remote Sensing Letters, Vol. 4, No. 3, 349–353, 2007.

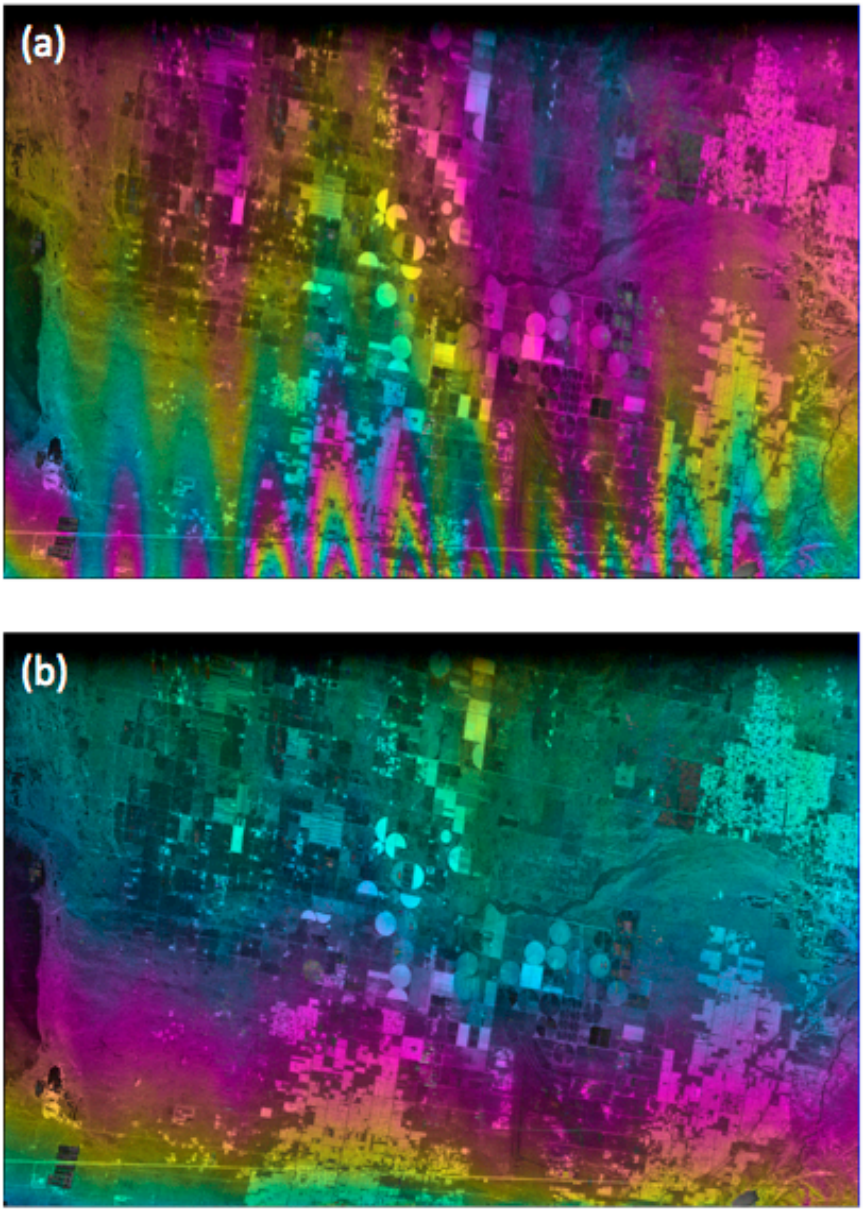

Fig. 6. *Repeat pass interferogram of an area in the Mojave Desert near Rosamond, California processed with the conventional motion compensation algorithm (a) and the advanced topography and aperture dependent motion compensation algorithm (b). The image swath is 17 km wide with the near range at the bottom of the image and the along-track direction from left to right. The phase wrap for the interferogram is set at* 2π *radians.*